JOURNAL OF GUIDANCE, CONTROL, AND DYNAMICS
Vol. 17, No. 2, March–April 1994

Base Reaction Control for Space-Based Robots Operating in Microgravity Environment

Roger D. Quinn* and Jiunn L. Chen†
Case Western Reserve University, Cleveland, Ohio 44106
and
Chuck Lawrence‡
NASA Lewis Research Center, Cleveland, Ohio 44135

Specialized robots are needed for space stations to conduct experiments and operations without disturbing the microgravity environment through base reactions and/or base motions. Approaches for controlling the robot base include 1) manipulators with redundant degrees of freedom, 2) actuators at the robot base, and 3) a redundant (balancing) arm. An approach making use of manipulator kinematic redundance is explored in detail and both locally and globally optimal trajectory management schemes are discussed. The inverse kinematic problem is solved at discrete time steps simultaneously with the minimization of the robot's base reactions. Numerical examples are presented including various robotic configurations and degrees of manipulator kinematic redundance. A significant reduction in base reactions is observed in each case.

I. Introduction

THE planned international Space Station Freedom will provide microgravity laboratories for basic research and manufacturing. Efficient and continuous utilization of these laboratories, as well as future capitalization of space, will depend on robotic manipulators for conducting experiments and performing processes. A unique requirement of these manipulators will be to operate without adversely disturbing the microgravity environment. To fulfill this specialized requirement, "reactionless" robotic systems are envisioned that provide experiment and manufacturing capability, specimen handling, and multipurpose transport in cooperation with human activity. These robotic systems will minimize crew member involvement in addition to permitting acceleration sensitive operations to be performed.

Two related control problems are associated with the operation of robots in a microgravity environment.[1] The first is the transportation of specimens without exceeding microgravity accelerations on the specimens themselves. The transportation of objects at microgravity acceleration levels requires precise trajectory planning for the robot's end-effector and, obviously, requires very slow manipulations. Optimal trajectory planning to minimize the mission time is clearly desirable.

Special attention also must be paid to the manipulator joint design, since conventional manipulators may not be able to operate smoothly enough to execute microgravity level maneuvers due to inherent friction, backlash, and torque ripple. A conventional industrial robot can perform, at best, milli-g manipulation, three orders of magnitude too large for microgravity requirements for space.[2] Specialized robotic joints, for instance, with traction-driven transmissions, have been proposed for overcoming this limitation, but experimental verification is not yet available.[3-7]

The second control problem is associated with the operation of the robot without transmission of dynamic disturbances to the surrounding environment. For every motion of the manipulator there will be a counteracting reaction at the manipulator base. If these reactions are not controlled, they may be transmitted to the laboratories where they may disturb the microgravity environment. Earth robots often employ massive bases to act as reaction masses, eliminating base motions and absorbing base reactions during the robot's operation. Space-based robots may not have this luxury due to orbital mass minimization requirements. Hence, the base motions must be eliminated or controlled by other means. The simplest solution for reducing base reactions is to move the robot arm slowly. For situations that permit high accelerations at the end-effector, such as the transportation of nonsensitive test equipment, swifter motions are desirable. Under this condition, devices or specialized trajectory planning strategies that compensate for the resulting base reactions must be employed. If the robot is free-floating, then similar strategies could be used so that the motion of the base does not obstruct, or collide with, other activities.

This paper is concerned with methods of reducing base reactions/motions of space-laboratory robots so that they may operate without transmission of significant dynamic disturbances to the surrounding environment. The application and performance assessment of trajectory planning strategies for minimizing the base reactions of kinematically redundant robots is discussed in detail. In Sec. II, the robot dynamics and the ensuing base reactions are discussed. In Sec. III, two alternate methods for base reaction control, actuation at the robot base and a balancing arm approach, are discussed. In Sec. IV, another method of base reaction control involving the use of kinematically redundant manipulators is pursued in detail. Two trajectory planning strategies, one using a local optimization approach and the other a global approach, are discussed. An implementation of the local approach is detailed. Section V presents results, using the local approach, for both two- and three-dimensional robot manipulators with varying degrees of kinematic redundancy. The performance of the local optimization approach is assessed.

II. Robot Dynamics

A typical robotic task requires transporting an object gripped by the end-effector through a trajectory. The object (assumed to be rigid) has six degrees of freedom, so the

Presented as Paper 88-4121 at the AIAA Guidance, Navigation, and Control Conference, Minneapolis, MN, Aug. 15-17, 1988; received Jan. 4, 1991; revision received Feb. 19, 1993; accepted for publication March 2, 1993.

*Associate Professor, Department of Mechanical and Aerospace Engineering. Member AIAA.
†Graduate Research Assistant, Department of Mechanical and Aerospace Engineering.
‡Aerospace Engineer. Member AIAA.

manipulator must have at least six degrees of freedom provided by its joints to orient and position the object arbitrarily in space.

The equations of motion may be developed in terms of the n joint coordinates and six coordinates representing the base motion. If the base motion is then specified as null, the resulting base reactions are obtained. The equations of motion in general form may be expressed in terms of the n joint coordinates as

$$M(q)\ddot{q} + C(q, \dot{q}) = \begin{bmatrix} Q_0 \\ Q \end{bmatrix} \tag{1}$$

where M is an $(n+6) \times n$ inertia matrix and C is an $(n+6) \times 1$ vector of Coriolis and centrifugal terms, $Q_0^T = [F_B^T \quad M_B^T]$ and Q are the vectors of forces and moments at the base and at the joints, respectively. For Earth-based robots, many of the Coriolis and centrifugal terms are relatively small and often are neglected.[8] However, for space-based robots, these terms may be significant, particularly relative to microgravity level accelerations.

Let p be a set of six variables describing the position and orientation of the end-effector, and let q be a set of n variables describing the joint configuration. The relationship between p and q depends on the kinematics of the manipulator. In general, the path variable p is a nonlinear function of the joint variables q or

$$p = p(q) \tag{2}$$

Given the joint variables, Eq. (2) provides the corresponding end-effector position and orientation. However, in typical robotic applications, the end-effector path is specified and the corresponding joint variables must be determined. This problem is known as the inverse-kinematics problem since it requires the inversion of Eq. (2). In general, this inversion is not straightforward because Eq. (2) is nonlinear.

The inverse-kinematics problem is more easily solved in differential or velocity form. Differentiating Eq. (2) with respect to time, the velocity form of Eq. (2) can be expressed as

$$\dot{p} = J(q)\dot{q} \tag{3a}$$

where the Jacobian matrix is defined as

$$J_{ij} = \frac{\partial p_i}{\partial q_j}; \quad i = 1, 2, 3, \ldots, 6, \quad j = 1, 2, 3, \ldots, n \tag{3b}$$

If $n = 6$, the Jacobian is square and the inverse of Eq. (3a) is straightforward, assuming that the Jacobian is nonsingular. If $n > 6$, then there are redundant degrees of freedom in the manipulator and an infinite number of solutions exist. In this case, a particular solution may be chosen on the basis of an optimization strategy.[8]

III. Base Control Using Actuation at Robot Base or Balancing Arm[1]

The most straightforward method of base motion/reaction control is to provide actuators at the base that supply forces and moments that cancel the reactions resulting from the robot motions. A combination of three-axis control moment gyros (CMG) and three-axis proof mass actuators (PMA), theoretically, can nullify the base moments and forces. The CMG may be eliminated by using the proper combination of six PMAs.

Control strategies that nullify base reactions also produce null acceleration of the base when the base is not attached to the space station. Controlled base motion is essential to enable free-flying robots to perform precise manipulations. Hence, the control schemes for minimizing base reactions are equally applicable for free-flying robots. If, in addition, thrusters are provided at the base, theoretically the robot can become mobile for use throughout the laboratory.

Control algorithms for actuators positioned at the base are relatively straightforward because the manipulator control problem may be performed independently of the base control. The base control forces and torques follow directly from the manipulator dynamics once its task has been defined. First, the manipulator task is planned and the inverse-kinematics problem is solved to obtain the necessary joint motions. The manipulator dynamics then are used to determine the reactions at the base. Finally, the base actuators are used to negate the base reactions. An additional closed-loop control strategy could be implemented to fine-tune the performance. Although this approach is relatively straightforward, it does require that additional mechanisms and, therefore, mass be added to the system. If CMG and PMA are used, the momentum management of these devices then becomes an additional problem and drawback to this approach.

Instead of actuators at the robot base, a redundant arm sharing a common base with the worker manipulator arm may be used as a dynamic counterbalance mechanism. In normal walking, humans use their arms in this way to maintain balance and reduce joint loads. When reactionless operation is necessary, the balancing arm can move so as to produce equal and opposite base reactions of the worker arm, nullifying the net base reactions. So that all forces and moments are controllable, the balancing arm must have at least six degrees of freedom. When the balancing arm is not needed for counterbalancing, it can act as a second worker arm, increasing the task adaptability of the robotic system.

The block diagram of Fig. 1 illustrates a control strategy for a robotic system consisting of two manipulator arms where one of the arms (ARM2) acts as a counterbalance for the worker arm (ARM1). Output from ARM1's dynamic model includes the predicted base reactions, which are input to ARM2's inverse-dynamic model. The output from the latter block is joint motion of ARM2, which will cause base reactions opposite those of ARM1. This information is then input to the dynamic model of ARM2 to produce the necessary feedforward joint torques. The measured base reactions are then fed back to ARM2's controller for fine-tuning the dynamic balancing.

IV. Base Motion Control Using Trajectory Planning Strategies for Kinematically Redundant Robot Manipulators

A robotic manipulator is kinematically redundant if its number of degrees of freedom is greater than that required to accomplish the desired end-effector motion. As discussed in Sec. II, for manipulators having redundant degrees of freedom there are an infinite number of possible joint motion trajectories that will satisfy a specified end-effector motion. By utilizing an appropriate optimization strategy, the combination of joint motions that minimizes the resulting base reactions may be determined.

Quinn and Lawrence proposed the use of a particular performance function for minimizing base reactions for kinematically redundant space-based manipulators.[1] Essentially, the method entails using the kinematic redundancies to move parts of the manipulator dynamically opposite the other parts of the manipulator and end-effector, such that momentum is nearly conserved. The procedure employs an optimization strategy for identifying the joint motion solution set that minimizes the resulting base reactions. Figure 2 is a block diagram illustrating the method.

The trajectory planning problem is formulated for kinematically redundant manipulators where the cost is defined as the sum of the weighted squares of the base reactions or, in matrix form

$$G = F_B^T W_F F_B + M_B^T W_M M_B \tag{4}$$

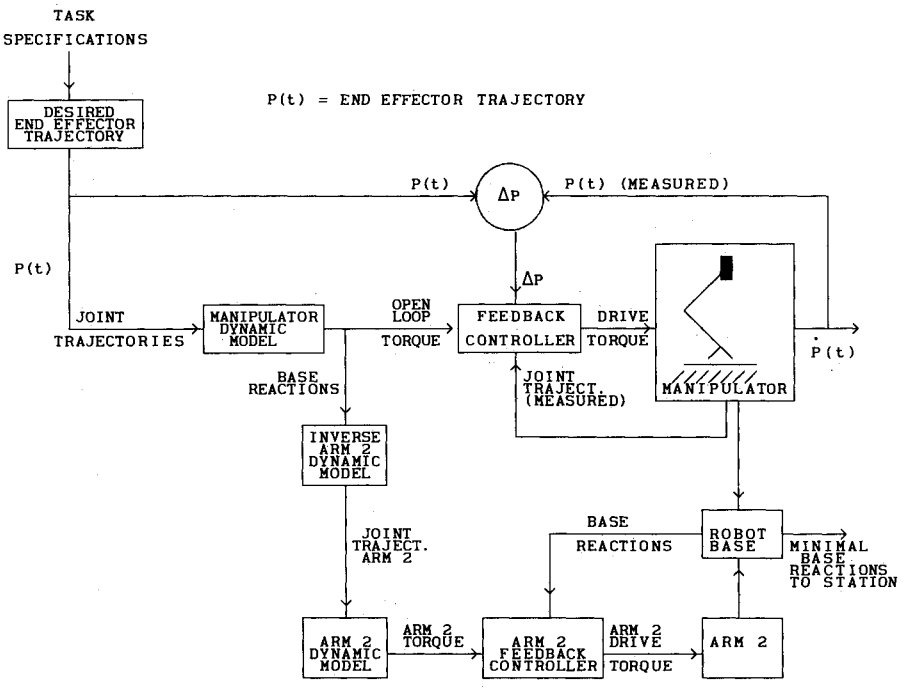

Fig. 1 Control strategy for robot with a redundant arm.

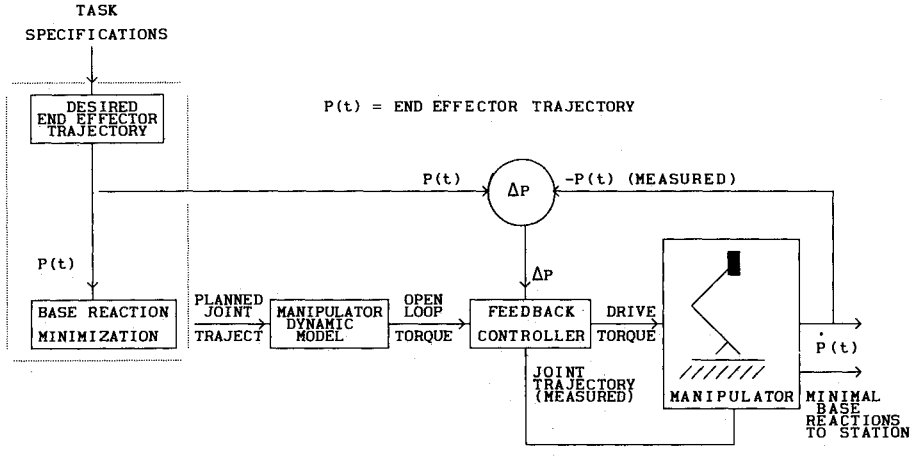

Fig. 2 Control strategy for manipulator with kinematic redundance.

where F_B and M_B are vectors of base forces and moments, respectively, and W_F and W_M are weighting matrices. Considering the manipulator dynamics described by Eq. (1), the quadratic cost function of Eq. (4) is a function of the joint variables and their time derivatives or

$$G = G(q, \dot{q}, \ddot{q}) \tag{5}$$

There are two types of tasks a manipulator must perform in robotic applications. One type requires the end-effector to follow a specified path, such as in arc welding. In the other type, the end-effector must move from one location to another, following no particular path, for example, transferring supplies or spot welding. In either case, the joint trajectories may be chosen to optimize a performance criterion, which will minimize the manipulator base reactions.

The cost function, Eq. (4), may be minimized at discrete time increments or integrated over the time of the entire trajectory path and then minimized. The former is referred to as the local approach because it involves local minimization of the base reactions, whereas the latter is referred to as the global approach because it entails global minimization over the entire trajectory. The local approach has been formulated for situations where the end-effector path is predefined, whereas the global approach has been formulated for cases where the entire end-effector path is defined, as well as when only the end-effector end points are specified.

A. Global Optimization

If the end points of the path, $p = p(t = 0)$ and $p = p(t = T)$, are specified but the path is not, Eq. (1) can be integrated over time, forming a cost functional, which can be expressed as

$$\hat{G}(q, \dot{q}, \ddot{q}) = \int_0^T (F_B^T W_F F_B + M_B^T W_M M_B)\, dt \tag{6}$$

The first variation of this functional yields a necessary condition for optimality, which can be expressed as

$$\delta\hat{G} = \int_0^T \left[\frac{\partial G}{\partial q}\delta q + \frac{\partial G}{\partial \dot{q}}\delta\dot{q} + \frac{\partial G}{\partial \ddot{q}}\delta\ddot{q} \right] dt = 0 \tag{7}$$

With the manipulator state specified at the end points, integration by parts leads to the Euler equations

$$\frac{d^2}{dt^2}\left(\frac{\partial G}{\partial \ddot{q}_i}\right) - \frac{d}{dt}\left(\frac{\partial G}{\delta \dot{q}_i}\right) + \frac{\partial G}{\partial q_i} = 0 \qquad i = 1, 2, \ldots, n \tag{8}$$

The solution of these n coupled ordinary differential equations is the time history of the n joints, which will produce an end-effector path that satisfies a necessary condition for minimizing the base reactions.

An approximate solution based on the Rayleigh-Ritz technique was introduced by Schmitt et al.[9] The joint variables are expressed as a linear combination of m admissible functions $\phi(t)$ satisfying the boundary conditions or

$$q = C\phi(t) \tag{9}$$

where C is a matrix of coefficients to be determined. Introducing Eq. (9) into Eq. (5), noting that the independent variables are now the coefficients of C, the necessary conditions for minimization of the cost can now be expressed as

$$\delta \hat{G} = \int_0^T \frac{\partial G}{\partial C_{ij}}\, dt = 0 \qquad i,j = 1, 2, \ldots, n \tag{10}$$

Since the time-dependent portions of Eq. (9) are known, it can be integrated producing $n \times m$ nonlinear algebraic equations to solve for the coefficients of the matrix C.

Chung and Desa used a global approach to minimize base reactions of a kinematically redundant manipulator where the end-effector path was specified.[10] Their solution method used the Rayleigh-Ritz method as shown previously, but the shape functions were partitioned into three sets that were valid at the beginning, middle, and end of the path, respectively. The partitioning of the joint trajectories into three sets reduces computational effort and maintains most of the advantages of the global optimization approach.

B. Local Optimization with Specified Path

If a manipulator has redundant degrees of freedom, the base reactions can be minimized even if the path is specified. In this case, the cost functional of Eq. (4) could be minimized subject to the six constraints expressed by Eq. (3a) where $p(t)$ is the prescribed position and orientation of the end-effector.[1]

DeSilva et al. presented a solution for the local trajectory planning problem by developing an optimization method for the trajectory design.[11] This solution entailed the evaluation of the cost function, Eq. (4), at discrete time increments along the trajectory path. The method is applicable to situations where the end-effector path is predefined. The base reactions and, hence, G are functions of the joint variables and their time derivatives as in Eq. (5).

From Eq. (3b), the Jacobian matrix is a $6 \times n$ matrix (n is larger than 6 for a redundant manipulator), and Eq. (3a) does not have a unique inverse-kinematic solution. As in the generalized inverse method, six of the joint variables are expressed as functions of the remaining $n - 6$ redundant joint variables based on Eq. (3a).[12] Hence, the variables in the cost function in the optimization scheme are reduced to the redundant joint variables only.

In the spirit of the generalized inverse method, the Jacobian matrix is partitioned into two matrices: one a nonsingular matrix, the other a redundant matrix. Similarly, the joint variables can be partitioned as nonsingular and redundant joint variables, which correspond to the nonsingular and redundant partitions of the Jacobian. Hence, Eq. (3a) can be expressed as

$$\dot{p} = J\dot{q} = [J_n \quad J_r]\begin{bmatrix}\dot{q}_n \\ \dot{q}_r\end{bmatrix} = J_n\dot{q}_n + J_r\dot{q}_r \tag{11}$$

where, in the most general three-dimensional case, J is a $6 \times n$ matrix, J_n is a 6×6 matrix, and J_r is a $6 \times (n-6)$ matrix. Also, $\dot{p}$ is a 6×1 vector, $\dot{q}_n$ is a 6×1 vector, and $\dot{q}_r$ is a $(n-6) \times 1$ vector. Taking the time derivative of Eq. (11), the acceleration of the end-effector can be expressed as

$$\ddot{p} = \dot{J}_n\dot{q}_n + \dot{J}_r\dot{q}_r + J_n\ddot{q}_n + J_r\ddot{q}_r \tag{12}$$

Since J_n is assumed to be nonsingular, the nonredundant variables in Eqs. (11) and (12) can be expressed in terms of the redundant variables and the specified end-effector trajectory or

$$\dot{q}_n = J_n^{-1}\dot{p} - J_n^{-1}J_r\dot{q}_r \tag{13}$$

$$\ddot{q}_n = J_n^{-1}\ddot{p} - J_n^{-1}\dot{J}_nJ_n^{-1}\dot{p} - J_n^{-1}J_r\ddot{q}_r + J_n^{-1}\left(\dot{J}_nJ_n^{-1}J_r - \dot{J}_r\right)\dot{q}_r \tag{14}$$

The joint trajectory at any arbitrary time can be expressed as the joint trajectory at the end of the previous time step plus the incremental joint motion during this time step or in equation form

$$q = q_0 + \begin{bmatrix}\delta q_n \\ \delta q_r\end{bmatrix} \tag{15}$$

where q_0 is the value of q at the previous time step. Substituting the variational form of Eq. (13) into Eq. (15) yields the following expression:

$$\begin{bmatrix}q_n \\ q_r\end{bmatrix} = \begin{bmatrix}q_n \\ q_r\end{bmatrix}_0 + \begin{bmatrix}J_n^{-1} \\ O\end{bmatrix}_0 \delta p + \begin{bmatrix}-J_n^{-1}J_r \\ I\end{bmatrix}_0 \delta q_r \tag{16}$$

Note that the subscript 0 implies values evaluated at the previous step at any arbitrary time t and I denotes an $(n-6) \times (n-6)$ identity matrix. Therefore, the joint configuration can be obtained approximately from Eq. (16) in a step by step discrete-time approach.

Once the preceding steps have been completed the cost can be expressed as a function of the redundant variables and their time derivatives, or $G(q_r, \dot{q}_r, \ddot{q}_r)$. Up to this point, the solution developed by deSilva has followed the generalized inverse method. However, to avoid the difficulty of finding the functions of time denoted by q_r, the local optimization method now makes use of the Rayleigh-Ritz technique. In this way the redundant joint variables are transformed to a new set of independent variables using shape functions, which are time dependent. In the optimization scheme, the new set of independent variables are chosen to minimize the cost function.

The Rayleigh-Ritz technique is used to discretize the joint trajectories in time. Let the time derivatives of the redundant joint variables be expressed as

$$\dot{q}_r(t_i + \tau) = \Re f(\tau) \tag{17}$$

where $0 < \tau < \Delta t$, $\Delta t = (t_{i+1} - t_i)$ and $\dot{q}_r$ is an $(n-6) \times 1$ vector; $\Re$ is an $(n-6) \times m$ matrix of unknown coefficients; $f(\tau)$ is a known set of m shape functions that is used to represent the variation of $\dot{q}_r$ within a trajectory time step. The shape functions are chosen as the set of polynomials

$$f(\tau) = [1, \tau, \tau^2/2!, \ldots, \tau^{m-1}/(m-1)!]^T \tag{18}$$

Taking the time derivative of Eq. (17), the redundant joint acceleration equation becomes

$$\ddot{q}_r = \Re \dot{f}(\tau) \tag{19}$$

Furthermore, inserting the variational form of Eq. (17) into Eq. (16), the joint variables can be expressed as

$$\begin{bmatrix} q_n \\ q_r \end{bmatrix} = \begin{bmatrix} q_n \\ q_r \end{bmatrix}_0 + \begin{bmatrix} J_n^{-1} \\ O \end{bmatrix}_0 \delta p + \begin{bmatrix} -J_n^{-1}J_r \\ I \end{bmatrix}_0 \Re f(\tau)\delta t \qquad (20)$$

where δt is the time difference for each trajectory segment. The cost can now be expressed as a function of the coefficients of the matrix $\Re$ or $G = G(\Re)$.

Because of the complexity of the cost function equation, formulating its gradients is difficult. Hence, numerical methods, such as Powell's method with no numerical computation of the gradient or the quasi-Newton method with the gradient determined by numerical differentiation, are required.

Given the initial joint configuration, a numerical optimization scheme produces the matrix $\Re$ of Eq. (17), which, at the beginning of each time step, minimizes the base reactions evaluated at the end of the time step or

$$\min[F_B^T W_F F_B + M_B^T W_M M_B]_{\tau = \Delta t} \qquad (21)$$

given the initial dynamic state and the kinematic path constraints. The joint variables at the next time step are computed using Eqs. (17) and (20). This procedure is repeated until the end-effector reaches the final configuration.

C. End Effector Trajectory Generation

An important step in limiting base reactions is permitting only smooth, finite jerk end-effector motion whenever possible. Curtate cycloidal motion is used because it is well known that it has the desired properties of limited acceleration and jerk.

For the purposes of the numerical examples that follow, straight line end-effector motion from a specified starting position and orientation to a specified final configuration are considered. The end-effector is specified to move along a straight line and rotate so that the required orientation can be reached at the final point of the path.

Let the direction of the straight line path be denoted by the unit vector $\boldsymbol{u}$ and the position of the end-effector along this path be $y(t)$. Also, let the unit vector $\boldsymbol{K}$ denote the direction of the axis of rotation and the angle of rotation be defined as $\theta(t)$. Then both the linear and angular velocities of the end-effector can be expressed as[13]

$$\dot{p} = \begin{bmatrix} \dot{y}\boldsymbol{u} \\ \dot{\theta}\boldsymbol{K} \end{bmatrix} \qquad (22)$$

According to curtate cycloidal motion, both $y(t)$ and $\theta(t)$ are varied and synchronized with respect to the time variable. The time t and the end-effector motion can be expressed in terms of a new parameter ρ as

$$t(\rho) = k[\rho - c\sin(\rho)] \qquad (23)$$

$$\dot{y}(\rho) = b_1[1 - \cos(\rho)] \qquad (24)$$

$$\dot{\theta}(\rho) = b_2[1 - \cos(\rho)] \qquad (25)$$

where k, b_1, $b_2 > 0$, $1 > c > 0$, and $2\pi \geq \rho \geq 0$. The linear and angular velocities of the end-effector are zero at the starting point, $\rho = 0$, and at the final point, $\rho = 2\pi$. The maximum accelerations and jerks occur at $p = \cos^{-1}(c)$ and $p = 0, 2\pi$, respectively. Parameters b_1, b_2, and c can be chosen to satisfy the desired acceleration and jerk limits.

V. Numerical Results

A generalized computer formulation based on the local optimization approach was developed to examine the effectiveness of the base reaction minimization strategy. The formulation is general in that two- or three-dimensional robotic manipulators with any number of link and revolute joint combinations may be considered, and the end-effector path can be specified as either translational only or translational and rotational. Note that the dimensionality of the nonredundant joint variables varies according to the dimensionality of the robot motion. For example, a planar robot, with both translation and rotation of the end-effector specified, must have three nonredundant joint variables.

The inputs to the computer model include the robotic link geometries and inertia properties and joint degrees of freedom. The links are assumed to be rigid. The input for the end-effector trajectory includes the initial and final configuration of the end-effector, its maximum permitted acceleration, total excursion time, and number of discrete time steps. The initial joint configuration also must be specified. A straight line end-effector path is assumed between end points.

In each case, the objective is to determine the joint trajectories of the robot that will cause the end-effector to follow the desired path and minimize its base reactions. The shape functions are chosen as in Eq. (19) with $m = 3$ (constant jerk). The paths are divided into 20 equal time steps and dimensions are in Newtons, meters, and seconds. It was found that an increase in the number of time steps caused the sharp peaks in base reactions to be smoothed and slightly reduced. The base reactions are evaluated and minimized at the end of each time step. The quasi-Newton method (with a numerical calculation of the gradient) was found to be a reliable method of optimization for this purpose. The following plots of reactions vs

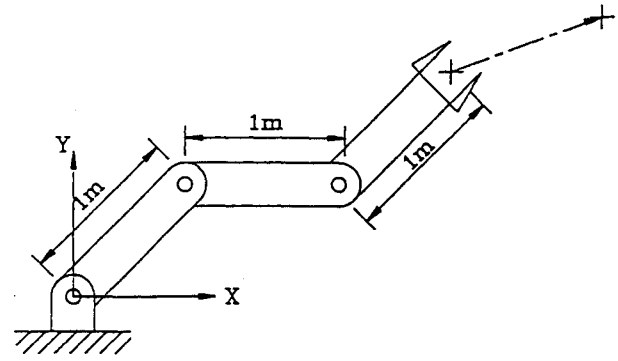

Fig. 3 Three-degree-of-freedom planar robot for example 1.

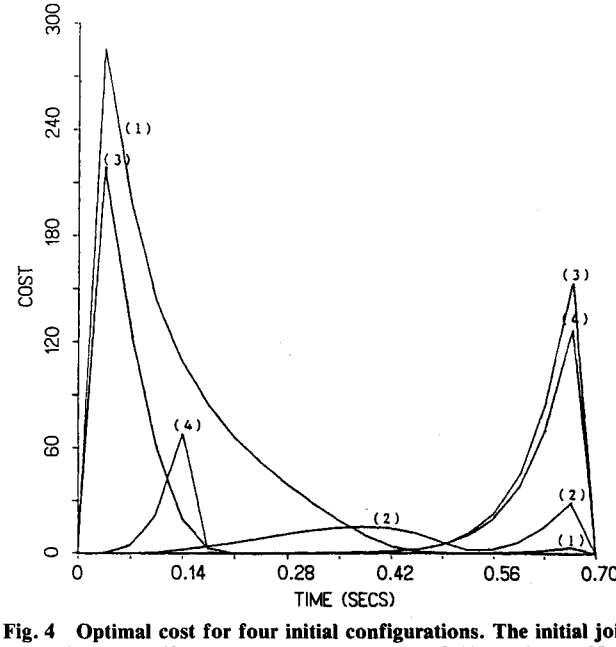

Fig. 4 Optimal cost for four initial configurations. The initial joint angles [$q1$, $q2$, $q3$] in degrees are as follows: 1) [108, −72.1, −38.1]; 2) [85.1, −24.2, −82.1]; 3) [62.2, 21.7, −106.1]; and 4) [33.5, 75.9, −109.1].

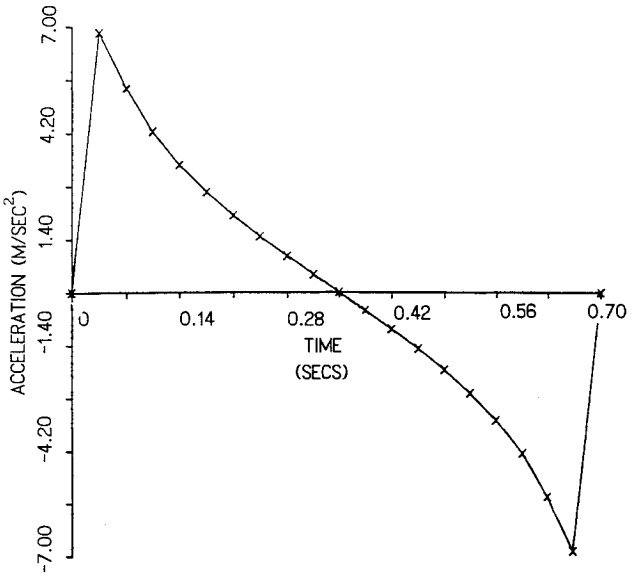

Fig. 5 End-effector acceleration for example 1.

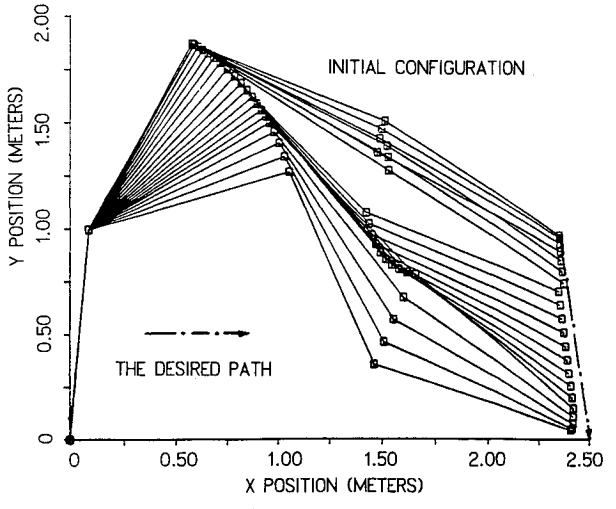

Fig. 6 Time-lapse plot showing optimal link trajectories for example 2.

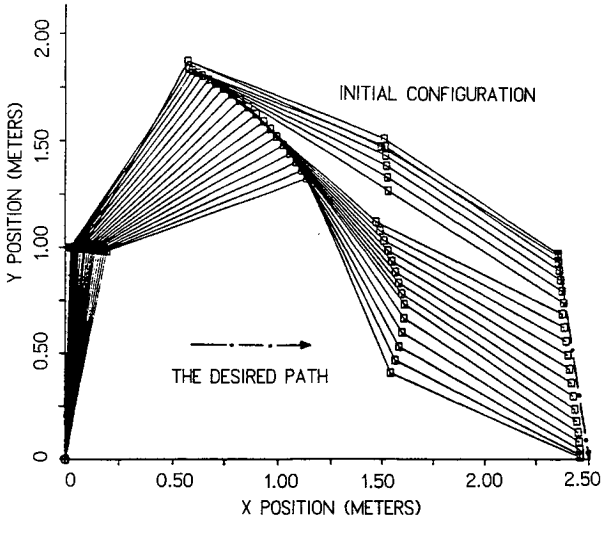

Fig. 7 Time-lapse plot showing optimal link trajectories for example 3.

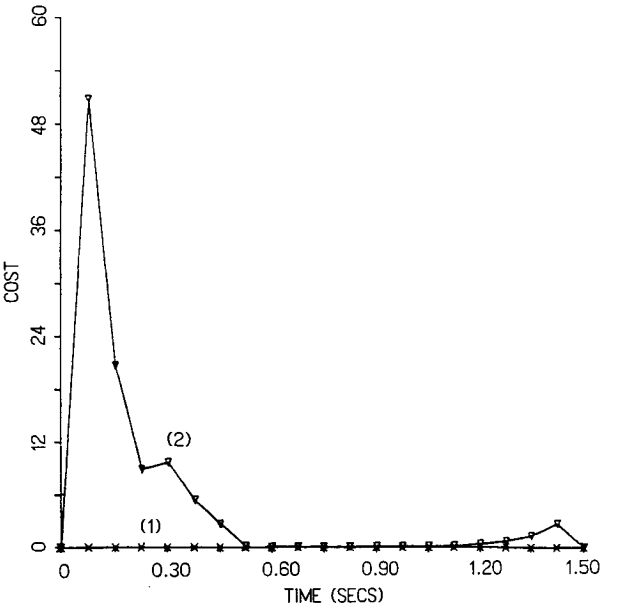

Fig. 8 Base reaction performance vs time for examples 2 and 3. Curve 1 corresponds to example 3 and curve 2 corresponds to example 2.

time show only the reactions evaluated at the end point of each time step.

A. Two-Dimensional Examples

In part 1, only translation of the end effector is specified, whereas in part 2, both translation and rotation are considered.

1. End-Effector Translational Path Specified

In example 1, consider a three-degree-of-freedom planar manipulator (Fig. 3) that has 1 deg of redundancy when only translation of the end effector is specified. The three slender links are identical. Each uniform link is 1 m in length, 1 kg in mass, and its mass moments of inertia are $I_{xx} = 0$ and $I_{yy} = I_{zz} = 0.75$ kg-m^2 in link coordinates. The desired path in (x, y) coordinates and meters is from (2.5, 2.5) to (3.0, 3.0), and the maximum acceleration is 7 m/s^2. The initial joint angle configuration $q1$, $q2$, $q3$ (relative coordinates) is given as 85.1, -24.2, and -82.7 deg, respectively.

The effectiveness of the use of kinematic redundancy for base reaction minimization depends on the initial joint configuration of the manipulator (see Fig. 4). The results for this figure were generated by specifying four different initial joint configurations (the end-effector trajectory is identical in each case). A comparison of these plots with a plot of end-effector acceleration vs time shown in Fig. 5 demonstrates the correlation between peaks in acceleration and cost. This correlation shows the importance of limiting end-effector acceleration for base reaction reduction.

Consider a four-degree-of-freedom robot constructed similarly to the one in Fig. 3 but with an additional 1 m long slender link. All four links have the same geometry and inertia as in example 1. The initial relative joint angle configuration $q1$, $q2$, $q3$, $q4$ is given as 85.1, -24.2, -82.1, and -11.5 deg, respectively, which is illustrated in Fig. 6. The maximum acceleration of the end-effector is given as 6 m/s^2. Examples 2 and 3 are similar except that in example 2 the first joint is fixed, resulting in only one redundant degree of freedom. In example 3, all joints are permitted to move, thus the manipulator has two redundant degrees of freedom.

Figures 6 and 7 are time-lapse plots of the manipulator configuration at several time steps during the maneuver for examples 2 and 3, respectively. The desired path of the end-effector is illustrated by the dashed line and arrow. The desired end-effector path is not followed precisely because of the

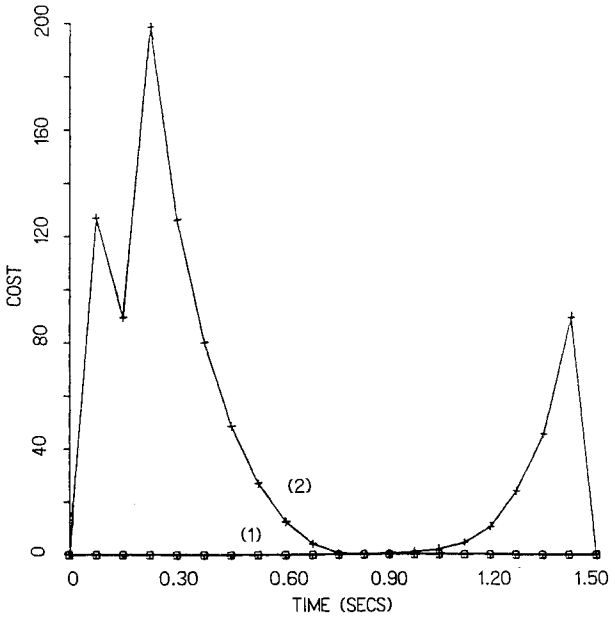

Fig. 9 Base reaction performance vs time for examples 4 and 5. Curve 1 corresponds to example 5 and curve 2 corresponds to example 4.

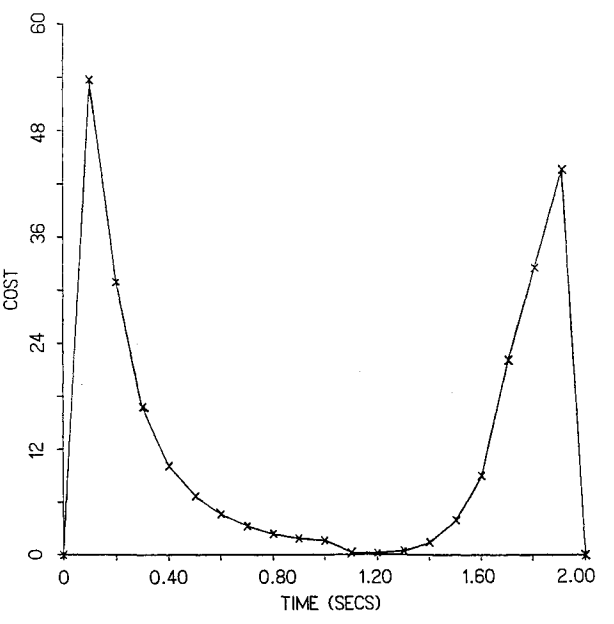

Fig. 11 Base reaction performance vs time for example 6.

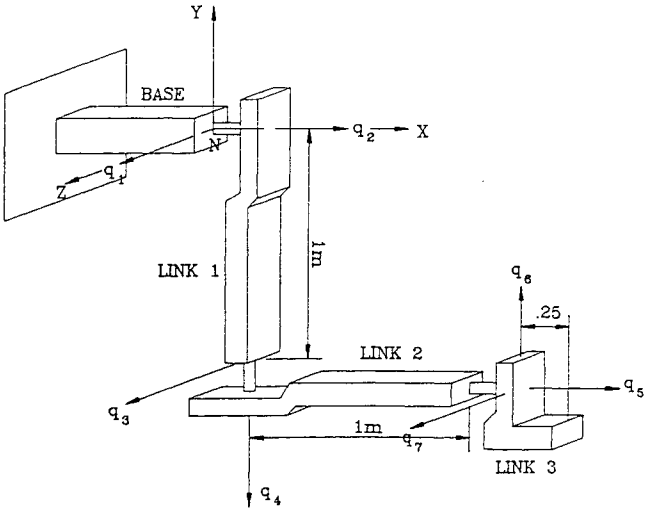

Fig. 10 Seven-degree-of-freedom spatial manipulator.

discrete-time error in this open-loop control approach. Reducing the step size reduces this error.

Figure 8 is a comparison of the cost vs time for examples 2 and 3. Clearly, the additional redundant degree of freedom of the manipulator of example 3 is highly advantageous in reducing the base reactions. Note that the base reactions in example 3 are not eliminated entirely but are negligible in comparison to example 2. Typical nonoptimal cases were considered for comparison where the Ritz coefficients were maintained as constants throughout the maneuver. In this case, the cost was found to be typically at least an order of magnitude larger than that of example 2 and two orders of magnitude larger than that of example 3.

2. Translational and Rotational Path Specified

Consider a five-degree-of-freedom manipulator constructed similarly to Fig. 3 but with two additional links, one of length 1 m and the last of length 0.25 m. Both translation and rotation of the end-effector path are to be specified. Specifically, the end-effector is to remain horizontal while following the specified straight line path. The first four links have the same geometry and inertia of those of examples 2 and 3. Link 5 is uniform, has a mass of 2 kg, a length of 0.25 m, and $I_{xx} = 0$, and $I_{yy} = I_{zz} = 0.281$ kg-m^2, all in link coordinates. The initial joint angle configuration $q1$, $q2$, $q3$, $q4$, $q5$ is 85.1, −24.2, −82.1, −5.73, and 26.91 deg, respectively. The maximum acceleration of the end-effector was chosen as 10 m/s^2. As in examples 2 and 3, examples 4 and 5 are similar except that in example 4, the first joint is fixed. Figure 9 is a comparison of the cost vs time for examples 4 and 5. As with the previous examples, the additional redundancy is very effective in reducing the base reactions.

B. Three-Dimensional Example

Example 6 is a seven-degree-of-freedom, three-link robot working in three-dimensional space. Joint degrees of freedom are depicted on Fig. 10 by the joint variables $q1, q2, \ldots, q7$. The first two links have the same geometry and inertia as the manipulator in example 1. Link 3 has the same properties as link 5 in examples 4 and 5. In this task, it is desired that the end-effector move linearly from position (0.38, 0.62, 0.68) m and orientation (−0.47, 0.50, 0.73) radians to (0.20, −0.5, 0.2) m and (1.0, 0.0, 0.0) radians in 2 s with a cycloidal trajectory and a maximum translational acceleration of 2 m/s^2 and maximum rotational acceleration of 3.351 rad/s^2. Because both translation and rotation of the end-effector path are specified there is only one redundant degree of freedom. A plot of the optimal cost function versus time is shown in Fig. 11. Again, note the peaks near the start and end of the motion, which correspond to the peaks in acceleration of the cycloidal trajectory.

VI. Conclusions

The use of kinematic redundancy for robot base reaction reduction has been explored in detail. Both global and local optimization approaches are discussed. In view of the apparent computational complexity of the global approach, we have chosen to consider the local approach with hopes of computational speeds that enable real-time control. A local point-to-point trajectory management strategy, where the reactions are minimized at the end of each time step and the end-effector path constraints are satisfied, appears promising. Numerical examples demonstrate that this approach is effective for reducing base reactions for planar and spatial manipulators. It is shown that by incorporating additional kinematic redundancy, the manipulator has more freedom of motion, and a

much greater reduction of base reactions may be achieved. The effectiveness of manipulator kinematic redundancy for base reaction reduction depends on the robot's initial configuration and the specified end-effector motion. Maximum base reactions are typically concurrent with maximum acceleration of the end-effector. Hence, limiting end-effector acceleration is important for reducing base reactions.

Acknowledgment

This work was supported by NASA Grant NAG3-797.

References

[1]Quinn, R. D., and Lawrence, C., "Robots for Manipulation in a Micro-Gravity Environment," *Sixth Virginia Polytechnic Institute and State University/AIAA Symposium on Dynamics and Control of Large Structures,* June–July 1987.

[2]Rohn, D. A., Lawrence, C., and Brush, A. S., "Microgravity Robotics Technology Program," Instrument Society of America, ISA/88 International Conference and Exhibit, Houston, TX, ISA Paper 88-1642, Oct. 1988.

[3]Harmon, P. E., and Rohn, D. A., "The Impact of an IVA Robot on the Space Station Microgravity Environment," *Proceedings of the NASA/Army Space and Military Applications of Robotics Conference*, Huntsville, AL, June 21–23, 1988, p. 4.

[4]Dodd, W. R., Badgley, M. B., and Konkel, C. R., "User Needs, Benefits, and Integration of Robotic Systems in a Space Station Laboratory," NASA CR-185150, Oct. 1989.

[5]Brush, A. S., "Microgravity Manipulator Demonstration," *Lewis Structures Technology '88,* NASA CP-3003-Vol. 1, May 1988, pp. 217–227.

[6]Lowenthal, S. H., Rohn, D. A., and Steinetz, B. M., "Application of Traction Drives as Servo Mechanism," *19th Aerospace Mechanisms Symposium,* NASA Ames Research Center, NASA CP-2371, May 1985, pp. 119–140.

[7]Kuban, D. P., and Williams, D. M., "Traction-Drive, Seven-Degree-of-Freedom Telerobot Arm: A Concept for Manipulation in Space," *21st Aerospace Mechanisms Symposium,* NASA Johnson Space Center, NASA CP-2470, May 1987, pp. 111–130.

[8]Asada, H., and Slotine, J. J. E., *Robot Analysis and Control,* Wiley, New York, 1986.

[9]Schmitt, D., Soni, A. H., Sirivasan, V., and Naganathan, G., "Optimal Motion Programming of Robot Manipulators," *Journal of Mechanisms, Transmissions, and Automation in Design,* Vol. 107, June 1985, pp. 239–244.

[10]Chung, C. L., and Desa, S., "A Global Approach for Using Kinematic Redundancy to Minimize Base Reactions of Manipulators Used in Microgravity Environments," *Proceedings of the 1989 ASME Design Technical Conference—15th Design Automation Conference*, Sept. 1989, pp. 297–303.

[11]deSilva, C. W., "Trajectory Design for Robotic Manipulators in Space Applications," *Journal of Guidance, Control, and Dynamics*, Vol. 14, No. 3, 1991, pp. 670–674.

[12]Goldenberg, A. A., Benhabib, B., and Fenton, R. G., "A Complete Generalized Solution to the Inverse Kinematics of Robots," *IEEE Journal of Robotics and Automation*, Vol. RA-1, No. 1, March 1985, pp. 14–20.

[13]Quinn, R. D., Chen, J. L., and Lawrence, C., "Redundant Manipulators for Momentum Compensation in a Microgravity Environment," *Proceedings of the AIAA Guidance, Navigation, and Control Conference,* AIAA, Washington, DC, 1988 (AIAA Paper 88-4121).